

GRZEGORZ DERFEL, MARIOLA BUCZKOWSKA  
JAKUB GUZOWSKI

Institute of Physics, Technical University of Łódź, ul. Wólczańska 219  
90-924 Łódź, Poland, e-mail: gderfel@p.lodz.pl

## DIELECTRIC AND FLEXOELECTRIC DEFORMATIONS INDUCED BY AC ELECTRIC FIELD IN INSULATING NEMATIC LAYERS

*The deformations of homeotropic nematic layers induced by ac electric field of frequency  $f$  were studied numerically. Two kinds of nematic liquid crystals with small negative dielectric anisotropy,  $\Delta\epsilon < 0$ , were considered: (i) the non-flexoelectric nematic, (ii) the nematic characterised by the positive sum of flexoelectric coefficients  $e = e_{11} + e_{33} > 0$ . It was found that at sufficiently low frequencies, the deformations varied with time. The deformations of purely dielectric nature had the period  $1/(2f)$ . The time period of flexoelectric distortions was equal to  $1/f$ . The influence of rotational viscosity and of thickness of the layer on the dynamics of deformations was analysed.*

**Keywords:** flexoelectricity, nematic layers, electric field induced deformations.

### 1. INTRODUCTION

The electric field induced deformations of nematic layers may have dielectric and flexoelectric origin since usually the nematic liquid crystals possess both dielectric anisotropy  $\Delta\epsilon$  and flexoelectric properties determined by the sum of flexoelectric coefficients  $e = e_{11} + e_{33}$  [1]. In both cases, the rise as well as the decay of deformations are characterised by specific rates which depend on the properties of the liquid crystal and on the parameters of the layer [2]. Therefore, if the layer is subjected to ac electric field, the director distribution varies periodically with time. The time evolution of the deformation depends on the field frequency  $f$ . In our previous paper, this effect was studied numerically in the homeotropically aligned nematic characterised by  $\Delta\epsilon = -0.7$  and  $e = 40 \text{ pCm}^{-1}$  [3]. The flexoelectric contribution vanished above a critical frequency and the deformation of dielectric nature stabilized at high frequencies.

In the present paper, the influence of the rotational viscosity, of the thickness of the layer and of the flexoelectric properties on the dynamics of deformations is analysed.

## 2. GEOMETRY AND ASSUMPTIONS

The homeotropic nematic layer of thickness  $d$  confined between two plates parallel to the  $xy$  plane of the coordinate system and placed at  $z = \pm d/2$  was investigated. The plates played the role of electrodes. Sinusoidally varying voltage with amplitude  $U_m = 20$  V and frequency  $f$ ,  $U(t) = U_m \sin 2\pi ft$ , was applied between them. The frequency was varied between 0.01 and 10 Hz. The interactions between nematic and boundary surfaces were determined by the anchoring strength parameter  $W$  equal to  $20 \times 10^{-6} \text{ Jm}^{-2}$ . A very pure electrically insulating nematic material was assumed. Its elastic properties were given by the elastic constants  $k_{11} = 6.2 \times 10^{-12} \text{ N}$  and  $k_{33} = 8.6 \times 10^{-12} \text{ N}$ . The rheological properties were expressed by rotational viscosity  $\gamma_1$  and by surface viscosity  $\kappa = 2.6 \cdot 10^{-8} \text{ Nsm}^{-1}$ . The backflow effect was neglected. Two different sets of parameters responsible for interaction with electric field were taken into account. They represented the non-flexoelectric nematic with low negative dielectric anisotropy  $\Delta\epsilon = -0.05$ , and the flexoelectric nematic characterised by  $\Delta\epsilon = -0.05$  and by the positive sum of flexoelectric coefficients  $e > 0$ .

## 3. METHOD

The director distributions,  $\mathbf{n}(z,t)$  were determined by the angles  $\vartheta(z,t)$  measured between  $\mathbf{n}$  and the  $z$  axis. They were obtained by numerical solving of the following set of equations [3]:

- equation of balance of elastic, viscous, dielectric and flexoelectric torques for the bulk

$$\begin{aligned}
& \frac{1}{2}(k_b - 1)\sin 2\vartheta(\zeta, t) \left( \frac{\partial \vartheta(\zeta, t)}{\partial \zeta} \right)^2 - (k_b \cos^2 \vartheta(\zeta, t) + \sin^2 \vartheta(\zeta, t)) \frac{\partial^2 \vartheta(\zeta, t)}{\partial \zeta^2} \\
& + \frac{1}{2} \frac{\varepsilon_0 \Delta \varepsilon}{k_{11}} \sin 2\vartheta(\zeta, t) \left( \frac{\partial V(\zeta, t)}{\partial \zeta} \right)^2 + \frac{1}{2} \frac{e_{11} + e_{33}}{k_{11}} \sin 2\vartheta(\zeta, t) \left( \frac{\partial^2 V(\zeta, t)}{\partial \zeta^2} \right) = \quad (1) \\
& = -\frac{\gamma_1 d^2}{k_{11}} \frac{\partial \vartheta(\zeta, t)}{\partial t}
\end{aligned}$$

where  $k_b = k_{33}/k_{11}$  and  $\zeta = z/d$ ;

- two equations of balance of elastic, viscous flexoelectric and anchoring torques for the boundaries

$$\begin{aligned}
& -\frac{1}{2} \frac{e_{11} + e_{33}}{k_{11}} \sin 2\vartheta(-1/2, t) \frac{\partial V(\zeta, t)}{\partial \zeta} \Big|_{-1/2, t} + \\
& + [k_b \cos^2 \vartheta(-1/2, t) + \sin^2 \vartheta(-1/2, t)] \frac{\partial \vartheta(\zeta, t)}{\partial \zeta} \Big|_{-1/2, t} + \quad (2) \\
& + \frac{1}{2} \omega \sin 2[\vartheta(-1/2, t)] = -\kappa \frac{d}{k_{11}} \frac{\partial \vartheta(-1/2, t)}{\partial t}
\end{aligned}$$

for  $\zeta = -1/2$  where  $\omega = Wd/k_{11}$  and

$$\begin{aligned}
& \frac{1}{2} \frac{e_{11} + e_{33}}{k_{11}} \sin 2\vartheta(1/2, t) \frac{\partial V(\zeta, t)}{\partial \zeta} \Big|_{1/2, t} + \\
& - [k_b \cos^2 \vartheta(1/2, t) + \sin^2 \vartheta(1/2, t)] \frac{\partial \vartheta(\zeta, t)}{\partial \zeta} \Big|_{1/2, t} + \quad (3) \\
& + \frac{1}{2} \omega \sin 2[\vartheta(1/2, t)] = -\kappa \frac{d}{k_{11}} \frac{\partial \vartheta(1/2, t)}{\partial t}
\end{aligned}$$

for  $\zeta = +1/2$ ;

- the Poisson equation

$$\begin{aligned} & \varepsilon_0 [\varepsilon_{\perp} + \Delta\varepsilon \cos^2 \vartheta(\zeta, t)] \frac{\partial^2 V(\zeta, t)}{\partial \zeta^2} - \varepsilon_0 \Delta\varepsilon \sin 2\vartheta(\zeta, t) \frac{\partial V(\zeta, t)}{\partial \zeta} \frac{\partial \vartheta(\zeta, t)}{\partial \zeta} \\ & + (e_{11} + e_{33}) \cos 2\vartheta(\zeta, t) \left( \frac{\partial \vartheta(\zeta, t)}{\partial \zeta} \right)^2 + \frac{1}{2} (e_{11} + e_{33}) \sin 2\vartheta(\zeta, t) \frac{\partial^2 \vartheta(\zeta, t)}{\partial \zeta^2} = 0 \end{aligned} \quad (4)$$

Boundary conditions for the potential had the form:  $V(-0.5, t) = 0$  and  $V(0.5, t) = U(t) = U_m \sin 2\pi ft$ . Stationary state of the deformations was ensured by imposing the periodic initial conditions:  $\vartheta(\zeta, 0) = \vartheta(\zeta, T)$  and  $V(\zeta, 0) = V(\zeta, T)$  where  $T = 1/f$ .

## 4. RESULTS

### 4.1. Non-flexoelectric nematic

In the case of the non-flexoelectric nematic, the director profiles  $\vartheta(z, t)$  have typical symmetric form and can be characterised by the mid-plane angle  $\vartheta(z = 0)$ . The time evolution of the deformation is shown in Fig. 1 where the angle  $\vartheta$  is plotted as a function of reduced time  $t/T$  and reduced coordinate  $\zeta$ . Figure 2 shows the time dependence of the mid-plane angle for several frequencies. It is evident that the deformation appears and disappears twice during the voltage cycle  $T = 1/f$ , therefore the time period of deformation equals to  $1/(2f)$ . This reflects the fact that the absolute value of the voltage and not the sign of the voltage is essential for the deformation of purely dielectric nature.

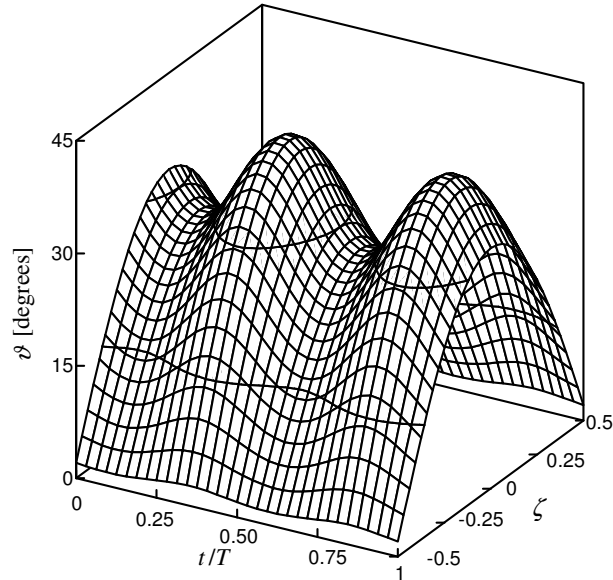


Fig. 1. The angle  $\vartheta$  plotted as a function of reduced time  $t/T$  and reduced coordinate  $\zeta$  for the non-flexoelectric nematic;  $d = 20 \mu\text{m}$ ,  $\gamma_1 = 0.076 \text{ Nsm}^{-2}$ ,  $f = 1 \text{ Hz}$

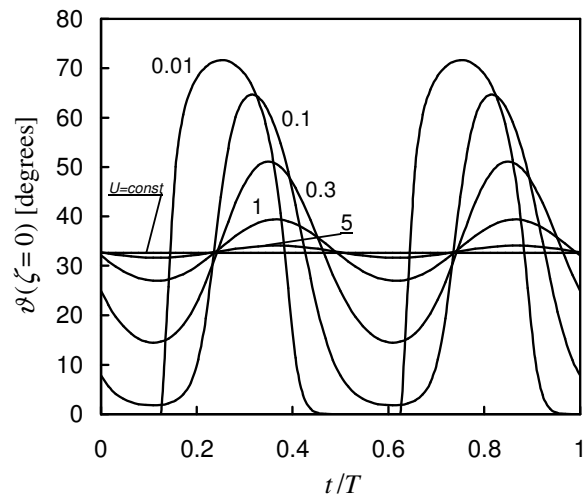


Fig. 2. The mid-plane angle  $\vartheta(0,t)$  plotted as a function of reduced time  $t/T$  for the non-flexoelectric nematic;  $d = 20 \mu\text{m}$ ,  $\gamma_1 = 0.076 \text{ Nsm}^{-2}$ . The frequencies in Hz are given at the curves. The horizontal line corresponds to static deformation obtained for  $U = U_m / \sqrt{2}$

For very low frequency,  $f = 0.01$  Hz, the deformation has a quasi-static character which is illustrated in Fig. 3. The time dependent voltage  $U(t)$  as well as the value of the dc threshold  $U_1$  are also plotted for comparison. It is evident that the deformation at the time  $t$  realized for  $f = 0.01$  Hz (curve) is very close to the static deformation obtained for the dc voltage equal to  $U = U(t)$  (squares). The quasi-static deformation starts when the voltage exceeds some value close to the dc threshold.

For higher frequencies, the time dependence of the angle takes the quasi-sinusoidal form. The amplitude of the quasi-sinusoidal variation of  $\vartheta(t)$  decays with frequency. This decay has an exponential form approximately. In order to characterize the dynamics of the deformations, the frequency  $f_\vartheta$  is introduced. It is defined as the frequency at which the amplitude of  $\vartheta(t)$  decays to 0.5 of its low frequency value. This frequency depends on the thickness of the layer as well as of the rotational viscosity of the nematic. (The corresponding calculations were performed for several sets of parameters determined by  $d = 10, 20$  and  $30 \mu\text{m}$  and  $\gamma_1 = 0.025, 0.050, 0.076$  and  $0.0100 \text{ Nsm}^{-2}$ ). Figure 4 shows that the frequency  $f_\vartheta$  is proportional to the quantity  $1/(\gamma_1 d^2)$  which is in agreement with analogous dependence of the time constants  $\tau$  for the rise and decay of the static Frederiks transitions,  $\tau \sim \eta d^2$ , where  $\eta$  denotes an effective viscosity [2].

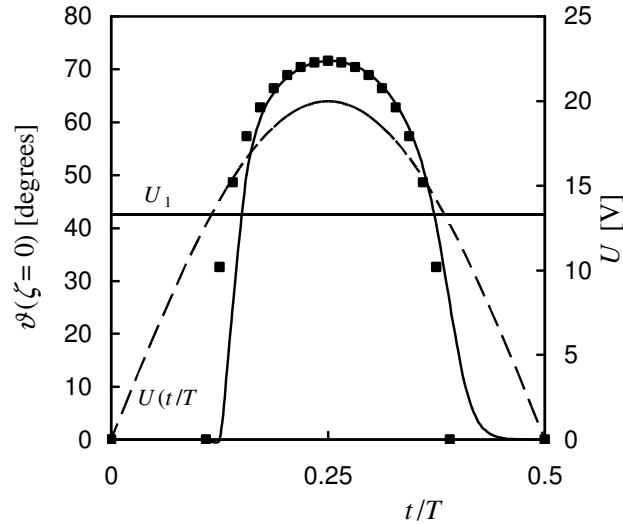


Fig. 3. The mid-plane angle  $\vartheta(0,t)$  (left scale) for  $f = 0.01$  Hz (continuous line) plotted as a function of reduced time  $t/T$  in comparison with the static deformation obtained at the same value of dc voltage (squares). Dashed lines: sinusoidal voltage and the dc threshold  $U_1$  (right scale).  $d = 20 \mu\text{m}$ ,  $\gamma_1 = 0.076 \text{ Nsm}^{-2}$

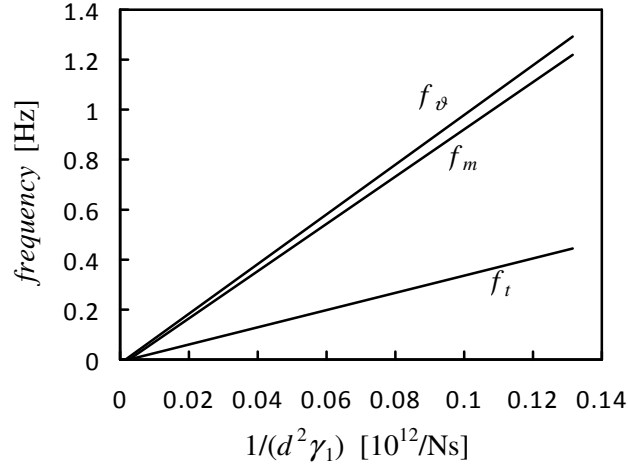


Fig. 4. The characteristic frequencies  $f_\delta$  and  $f_t$  for the non-flexoelectric nematic and the frequency  $f_m$  for  $e = 6 \text{ pCm}^{-1}$  plotted as a function of  $1/(d^2 \gamma_1)$

The maximum angle delays with respect to the voltage exhibiting an apparent inertia. The time interval  $\delta t$  which measures the delay is relatively short at  $f = 0.01 \text{ Hz}$ . It increases with frequency and saturates at high frequencies. The frequency  $f_t$  at which the half of the maximum  $\delta t$  is reached is another characteristics of the dynamics of deformation. As shown in Fig. 4, the value of  $f_t$  is also proportional to  $1/(\gamma_1 d^2)$  which confirms the role of rotational viscosity and thickness. When the frequency reaches sufficiently high values, the deformation tends to the stationary form corresponding to the rms value of the voltage  $U = U_m / \sqrt{2}$  [4].

## 4.2. Flexoelectric nematic

The flexoelectric nematic is characterised by the sum of the flexoelectric coefficients  $e$ . The calculations were performed for  $e = 6, 18$  and  $30 \text{ pCm}^{-1}$ . The director profiles  $\vartheta(\zeta, t)$  are asymmetrical as shown in Fig. 5 where the angle  $\vartheta$  is plotted as a function of the reduced time  $t/T$  and reduced coordinate  $\zeta$ . The deformation is characterised by the mid-plane angle  $\vartheta(\zeta = 0)$  and by the boundary angle  $\vartheta(\zeta = -0.5)$ . The time evolution of the deformation is shown in Figs. 6 and 7 for  $\zeta = 0$  and  $\zeta = -0.5$  respectively. It is evident that the time period of deformation equals to the voltage cycle  $T = 1/f$  due to flexoelectric

contribution which is a linear effect with respect to the electric field [5]. The flexoelectric torques manifest themselves in the subsurface deformations shown in Fig. 7. At low frequencies, the dielectric contribution gives rise to two maxima at the boundaries. Their magnitudes are different due to the flexoelectric torques. At  $\zeta = -0.5$ , the lower maximum appears in the first half of the voltage period and a higher maximum arises in the second half. However, the first maximum decreases when the frequency grows up and at sufficiently high frequency it merges with the first minimum. This means that the subsurface deformation is determined by the linear flexoelectric effect (curve for 10 Hz in Fig. 7). One may define a characteristic frequency  $f_m$  at which the difference between the first maximum and the first minimum decreases to half of its initial value. This frequency characterises the dynamics of the dielectric contribution. It is proportional to the quantity  $1/(\gamma d^2)$  as shown in Fig. 4. The frequency at which first maximum vanishes decreases with increasing  $e$ .

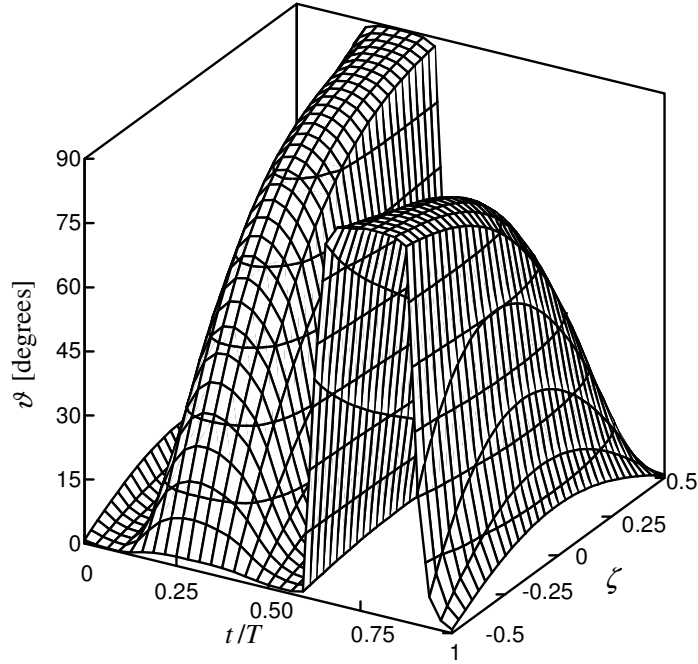


Fig. 5. The angle  $\vartheta$  plotted as a function of reduced time  $t/T$  and reduced coordinate  $\zeta$  for the flexoelectric nematic;  $e = 30 \text{ pCm}^{-1}$ ,  $d = 20 \text{ }\mu\text{m}$ ,  $\gamma_1 = 0.076 \text{ Nsm}^{-2}$ ,  $f = 0.1 \text{ Hz}$



## 5. SUMMARY

The above results show that in the considered layers containing nematic liquid crystals with rather small dielectric anisotropy, the deformation of dielectric nature becomes static at lower frequency than the deformation of flexoelectric origin. The dynamics of the dielectric deformations is governed by the quantity  $\gamma d^2$  in agreement with properties of the time constants responsible for the onset and decay of the Frederiks transitions.

The flexoelectric deformations can be caused by the torques in the bulk which are due to the gradient of the electric field and by the surface torques which depend on the electric field strength acting on the boundaries. In the considered case of insulating nematic, the field gradients are very small. The surface flexoelectric torque at the positive electrode are destabilizing, whereas the torque at the negative electrode quenches the deformation. The deformations in the bulk have dielectric origin and are remarkable in the case of  $e = 6 \text{ pCm}^{-1}$ . In the case of  $e = 30 \text{ pCm}^{-1}$ , the deformations are dominated by the director orientations forced at the boundaries by the surface flexoelectric torques.

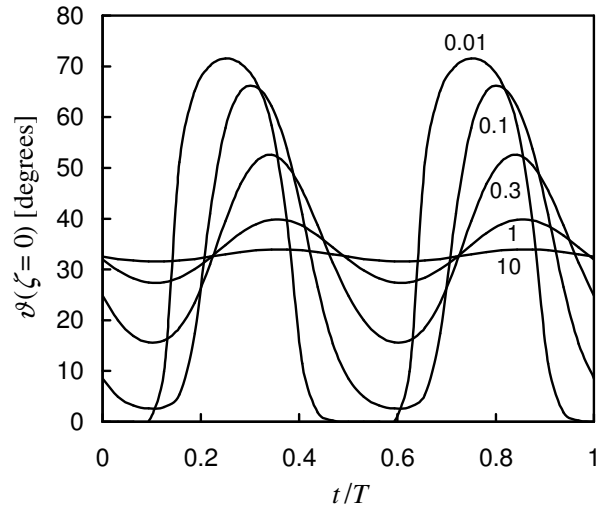


Fig. 6. The mid-plane angle  $\vartheta(0,t)$  plotted as a function of reduced time  $t/T$  for the flexoelectric nematic;  $e = 6 \text{ pCm}^{-1}$ ,  $d = 20 \text{ }\mu\text{m}$ ,  $\gamma_1 = 0.076 \text{ Nsm}^{-2}$ . The frequencies in Hz are given at the curves

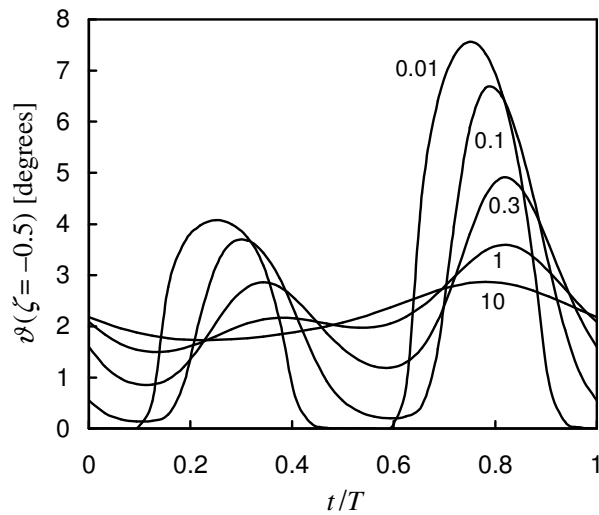


Fig. 7. The boundary angle  $\vartheta(-0.5, t)$  plotted as a function of reduced time  $t/T$  for the flexoelectric nematic;  $e = 6 \text{ pCm}^{-1}$ ,  $d = 20 \text{ }\mu\text{m}$ ,  $\gamma = 0.076 \text{ Nsm}^{-2}$ . The frequencies in Hz are given at the curves

## REFERENCES

- [1] **Blinov L.M., Chigrinov V.G.**, Electro-optic Effects in Liquid Crystal Materials, Springer Verlag, New York, 1993.
- [2] **Deuling H.J.**, "Elasticity of nematic liquid crystals", in: Liquid Crystals, Solid State Physics, Suppl. 14, pp. 103-107, edited by E. Liebert, Academic Press, New York, 1978.
- [3] **Derfel G., Buczkowska M.**, Opto-Electron. Rev., **19** (2011) 53.
- [4] **Gruler H., Cheung L.**, J. Appl. Phys., **46** (1975) 5097.
- [5] **Derzhanski A.I., Petrov A.G.**, Acta Phys. Pol., **A55** (1979) 747.

**DIELEKTRYCZNE I FLEKSOELEKTRYCZNE  
ODKSZTAŁCENIA WARSTW NEMATYCZNYCH  
WYWOŁANE ZMIENNYM POLEM ELEKTRYCZNYM**

**Streszczenie**

Zbadano numerycznie odkształcenia homeotropowych warstw nematyków wywołane zmiennym polem elektrycznym o częstotliwości  $f$ . Rozpatrzono dwa rodzaje nematycznego ciekłego kryształu o małej anizotropii dielektrycznej  $\Delta\epsilon < 0$ : nematyk pozbawiony właściwości fleksoelektrycznych oraz nematyk scharakteryzowany dodatnią sumą współczynników fleksoelektrycznych  $e = e_{11} + e_{33} > 0$ . Stwierdzono, że przy dostatecznie niskiej częstotliwości odkształcenie zmienia się okresowo z czasem. Okres deformacji czysto dielektrycznych wynosi  $1/(2f)$ , a deformacji o naturze fleksoelektrycznej równy jest  $1/f$ . Przeanalizowano wpływ lepkości rotacyjnej i grubości warstwy na dynamikę odkształceń.